

## Rotational viscosity in the smectic phases of terephthal-bis-butylaniline (TBBA)

S. Meiboom and R. C. Hewitt

Bell Laboratories, Murray Hill, New Jersey 07974

(Received 21 January 1977)

Measurements of rotational viscosity in the various liquid crystalline phases of TBBA (terephthal-bis-butylaniline) are reported. The quantity measured is the viscous energy dissipation in the liquid crystal as it oscillates in a magnetic field. This dissipation varies greatly in the different smectic phases. It is small in the *A* and *B* phases, but large and strongly temperature dependent in the *C* phase. This behavior is explained in terms of the structure of these phases. The smectic *A* to smectic *C* transition is of second order, and the dissipation increases dramatically at the transition point. The critical behavior is found to fit mean-field theory, rather than a predicted heliumlike behavior.

### INTRODUCTION

Nematic and smectic liquid crystalline phases exhibit a long-range orientational order: the long axes of the molecules are preferentially oriented along a specific direction, which will be referred to (for some phases somewhat loosely<sup>1,2</sup>) as the "director." An important consequence of this molecular alignment is that a magnetic or electric field will produce a torque on the director through the interaction of the field with the anisotropy of the magnetic or electric susceptibility, respectively. In nematics such effects are well known. For instance, the director will follow a slowly rotating magnetic field, resulting in a viscous drag which is detected as a torque on the sample. Such experiments were first described by Tsvetkov<sup>3</sup> some forty years ago. The hydrodynamics of nematic liquid crystals as formulated in the Leslie-Erickson equations<sup>4</sup> include such rotational effects. More recently, it has been shown<sup>5</sup> that reorientation of the director in smectic *C* can also be characterized by a rotational viscosity.

The work reported here was undertaken with the aim of investigating the effect of an applied director torque over a wider range of smectic phases. The compound chosen was TBBA [terephthal-bis-(4-*n*-butylaniline)]. This material has been quite extensively studied.<sup>6-17</sup> It exhibits a number of thermodynamically stable liquid crystalline phases: on cooling from the isotropic liquid it becomes successively nematic, smectic *A*, smectic *C*, and smectic *B<sub>c</sub>* (denoted by some authors as smectic *H*). The compound supercools easily to below the melting point, and at least two monotropic phases, VI and VII, are known to exist.<sup>7,11</sup> The temperature ranges of the different phases are indicated in Fig. 1.

Basically, the experiment consists of slowly

oscillating the liquid crystalline sample as part of the bob of a torsional pendulum placed in a magnetic field. The frequency and damping of the pendulum are measured as functions of temperature for all the phases mentioned above. It will be shown that dramatic changes in damping behavior occur at the transitions of one smectic phase to another. These changes can be correlated with the structure of these phases.

### EXPERIMENTAL

A schematic of the experimental setup is given in Fig. 2. The essential part is a torsional pendulum shown at the left of the figure. It consists of an open rectangular frame, about 60×4×4 mm, suspended between two thin gold ribbons, of the kind used in moving coil galvanometers; upper and lower ribbons are each about 50 mm long, 0.11 mm wide, and 0.006 mm thick. Inside the frame is a sealed glass tube containing 0.0504 g

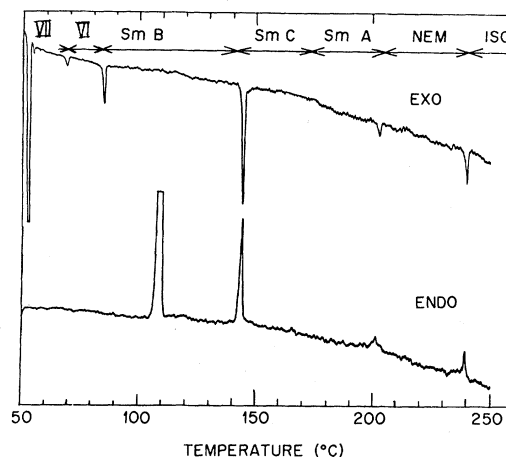


FIG. 1. Differential scanning calorimetry (DSC) traces of TBBA. Reproduced from Ref. 7.

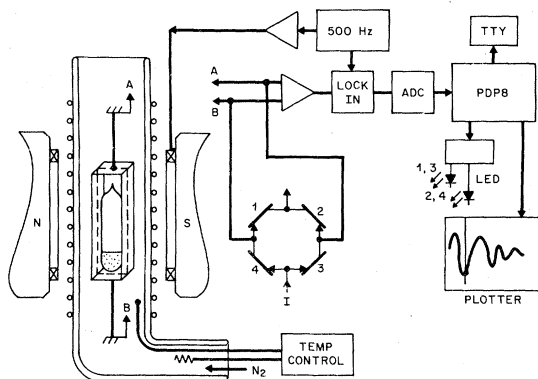


FIG. 2. Schematic diagram of the apparatus.

of the sample. Wound around the frame is a  $1\frac{1}{2}$ -turn coil of thin resistance wire. The gold ribbons serve as leads to this coil, electrical connection being made at the clamped ends of the ribbons as schematically indicated by A and B in Fig. 2. The pendulum has a natural oscillating period of about 1 sec. It is supported by a brass tube, not indicated in the figure, and is surrounded by a glass Dewar. A flow of heated nitrogen gas is used to control the temperature. Temperature sensing is done by a number of copper-Constantan thermocouples. To achieve better temperature uniformity, a heater element is wound on the outside of the Dewar, as indicated by the small circles in the figure. The current through this element is adjusted manually to a temperature near the desired one, so that heat transfer through the Dewar is minimized. The whole is placed inside the gap of a 12-in. Varian magnet, giving a field of 13.2 kG. It should be noted that the gold ribbon and the thin resistance wire of the coil are the only electrically conducting materials in the oscillating part of the pendulum. This is to keep eddy-current damping to a negligible value (see Appendix). In the original instrument, the frame was made up of thin glass strips, glued at top and bottom to small plastic blocks. In a later version, usable to higher temperatures, the separate frame is eliminated, and the suspensions and coil are made up of a single length of gold ribbon. This ribbon is supported directly by the glass tube containing the sample and kept in place by Teflon forms fitted to the top and bottom of the glass sample tube.

To operate the pendulum, two main functions are required: One is the measurement of the instantaneous position of the pendulum, and the second is a provision for applying suitable external torques in order to keep the pendulum in oscillation. The coil on the pendulum frame serves for both functions.

The setup for determining pendulum orientation is indicated in Fig. 2. It consists of a pair of modulation coils attached to the magnet poles, giving an alternating magnetic field of 500 Hz and a few gauss amplitude. This field induces a voltage in the pendulum coil, which is amplified and measured in a lock-in detector referenced to the ac of the modulation coils. The output of the lock-in detector is proportional to the sine of the angle between the plane of the pendulum coil and the direction of the modulation field. This output is digitized by the ADC (analog-to-digital converter) and stored in the memory of a PDP 8E computer for processing, as described below.

The pendulum is kept in oscillation by the application of current pulses to the pendulum coil, the duration of the pulses being short compared to the period. The current interacts with the main field of the magnet to give a torque pulse to the pendulum. The timing and duration of the excitation pulses is program controlled. In order to maintain symmetry, pulses of alternating sense are applied every third time the pendulum goes through its equilibrium position. A convenient way of applying the current pulses to the pendulum coil without interfering with the position measurements is the use of a bridge circuit made up of four phototransistors (1, 2, 3, and 4 of Fig. 2). The LED's of these transistors are switched on and off by the computer at appropriate times, alternating the 1, 3 with the 2, 4 transistors, in accord with the sense of the equilibrium crossing of the pendulum. The phototransistor bridge thus serves as gate and commutator for the constant current ( $i$ ) applied to the pendulum coil.

The measuring program for the computer is written in assembly language. It does the following functions:

(a) An interrupt applied every 0.01 sec by an external clock initiates a reading of the position ADC and its storage in memory. One thousand memory locations are allocated to position storage, each new reading overwriting the oldest number. Thus the memory always contains the one thousand most recent position readings, i.e., the history of the last ten or so oscillations. A display routine exhibits these data on a scope.

(b) Between interrupt services the program processes this history and keeps a running record of the oscillation amplitude and of the timing of the zero crossings. From this the timing and duration for the next pulse is calculated, and an output routine is activated at the right time to give the actual pulse. Pulse duration is determined by comparing the actual oscillation amplitude with the requested one (the latter is typed in at the start of the measurement). If the amplitude is

too low, pulse length is increased, if too large, pulse length is decreased. For stability, the feedback algorithm (in software) contains proportional, derivative, and integral terms in the amplitude deviation.

(c) On keyboard command, the computer will output the actual oscillation amplitude, period, and pulse length. The latter is directly proportional to the energy dissipation, while the period is related to the anisotropy of the magnetic susceptibility.

In a second measuring mode, the computer will, on command, stop outputting the current pulses, and plot the resulting decay of the oscillations on a *X-Y* recorder. A program, written in BASIC, will compute the exponential decay factor of the oscillations by a least-squares fit. This mode of operation is used mainly for calibration purposes as described in the next section.

The terephthal-bis-(4-*n*-butylaniline) (TBBA) was synthesized by refluxing phthaldehyde and *p*-butylaniline in ethanol. The product was recrystallized three times from a 1:1 mixture of benzene and petroleum ether. The final product had a melting point of 113.1 °C and a nematic to isotropic transition of 235.8 °C.

The sample used in the measurements was contained in a Pyrex glass tube, 4-mm o.d., 2.3-mm i.d., and 40 mm long. The TBBA was degassed by repeated freeze-thaw cycles under vacuum, and the sample was sealed off under vacuum. Weight of the TBBA was 0.0504 g. The moment of inertia of the pendulum, calculated from the dimensions and weights of the pendulum bob (mainly the glass tube containing the sample) was 0.0747 g cm<sup>2</sup>.

#### DATA REDUCTION AND CALIBRATION

In this section we collect a number of elementary equations used in interpreting the measurements. The apparatus is basically a pulse-driven harmonic oscillator. The observed quantities are oscillation amplitude, oscillation period, and pulse width. We wish to relate these quantities to the energy dissipation within the liquid crystal. It is convenient to introduce the quality factor  $Q$  and the dissipation  $D \equiv 1/Q$  of the oscillator. The quality factor is analogous to the well known  $Q = \omega L/R$  of an electrical *LC* circuit, and the same equations apply. The most useful here is

$$D \equiv \frac{1}{Q} = \frac{1}{2\pi} \frac{(\text{energy loss over one period})}{(\text{stored energy})}. \quad (1)$$

In the steady state the energy loss is made up by the energy delivered to the oscillator by the current pulses. The energy converted into me-

chanical energy by a pulse is

$$E_{\text{pulse}} = e_{\text{ind}} i \tau, \quad (2)$$

where  $i$  is the electrical current, and  $\tau$  the duration of the pulse;  $e_{\text{ind}}$  is the voltage induced in the moving coil by the magnetic field at the time of the pulse, i.e., when the oscillator goes through its equilibrium position. This voltage is proportional to the magnetic field strength ( $B$ ), the area of the moving coil ( $S$ ), and the angular velocity of the oscillator when going through the equilibrium position; the latter is in turn equal to the product of the amplitude ( $A$ ) and frequency ( $\omega$ ) of the oscillation. Thus

$$E_{\text{pulse}} = iBSA\omega\tau. \quad (3)$$

The stored energy in Eq. (1) can be calculated as the kinetic energy of the oscillator when going through the equilibrium position:

$$E_{\text{stored}} = \frac{1}{2}I(\dot{\phi})^2, \quad (4)$$

where  $I$  is the moment of inertia and  $\dot{\phi}$  is the angular velocity at the equilibrium position. As the latter equals  $A\omega$ , we get

$$E_{\text{stored}} = \frac{1}{2}I\omega^2A^2 \quad (5)$$

and Eq. (1) becomes

$$D = 1/Q = (CT/A)\tau, \quad (6)$$

where  $T = 2\pi/\omega$  is the period, and  $C$  contains the other factors ( $I, B, S, i$ ). The form of (6) has been chosen so that the quantities which vary during a set of measurements are written explicitly, while those that remain constant for a given sample have been absorbed in  $C$ . It is convenient to treat  $C$  as a calibration constant, and to determine it by observing the rate of decay of the oscillations in the nematic phase when the driving force is switched off. As will be discussed in the next section, the decay is exponential in the nematic phase. For this case, the number of periods in which the oscillation amplitude decays to  $1/e$  of its original value is equal to  $Q/\pi$ . The recording of such a decay is given in Fig. 3. The computer software includes a least-squares fitting routine to determine  $Q$  in this way. For the measurements reported here,  $C = 2.25 \times 10^{-3}$ , if the period is given in seconds, the amplitude in degrees, and the pulse length in the units used in the figures.

Two remarks are in order regarding the dissipation  $D$ . First, it is obvious from Eq. (1) that  $D$  is additive, i.e., the effect of two independent damping mechanisms is obtained by adding the  $D$ 's. Second, the definition of Eq. (1) is still useful in the more general case for which the damping term is not necessarily proportional to velocity,

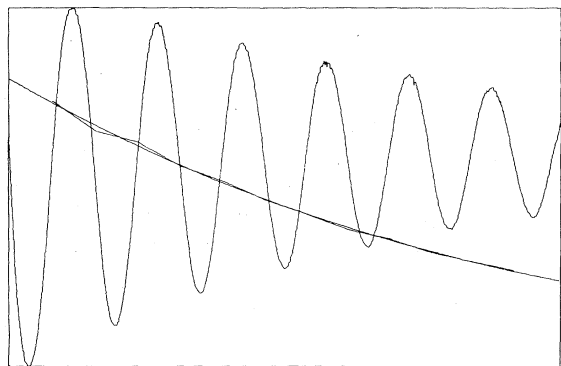


FIG. 3. Free decay of the pendulum when the sample is in the nematic phase. The temperature is 205.57°C. A computer program automatically determines the amplitude by taking the differences of the maxima and minima. A plot of these points, connected by straight lines, constitutes one of the two nearly overlapping curves. The second is an exponential least-squares fit to these points, also computed by the program.

as it is in the simple damped harmonic oscillator. In fact, it will be shown in the next section that the smectic *C* strongly deviates from this case. As long as the damping is not too large (i.e., as long as  $D \ll 1$ ), the oscillation is still nearly harmonic, and the above arguments relating  $D$  to pulse length still apply. However,  $D$  now becomes a function of oscillation amplitude.

We close this section with a short discussion of the factors which determine oscillation frequency. For a lightly damped torsional pendulum, the frequency is given by

$$\omega = (\Gamma/I)^{1/2}, \quad (7)$$

where  $I$  is the moment of inertia of the pendulum, and  $\Gamma$  the restoring torque per radian deviation. (This equation neglects the effect of the damping on the frequency, but is valid with good accuracy for the experiments reported here for which  $D \ll 1$ .) For a specific sample  $I$  is a constant, but the torque  $\Gamma$ , and therefore  $\omega$ , will vary with the liquid crystalline phase. There are two contributions to the restoring torque: the elastic torque of the pendulum suspension, and the magnetic torque on the liquid crystal. The latter is given by

$$T_m = \frac{1}{2}\chi_a WH^2 \sin 2\theta, \quad (8)$$

where  $\chi_a = \chi_{\parallel} - \chi_{\perp}$  is the diamagnetic anisotropy per unit mass of the liquid crystal,  $H$  the magnetic field strength,  $W$  the mass of the sample, and  $\theta$  the angle between the magnetic field and the principal axis of easy magnetization. Somewhat loosely, the latter can be identified with the direction of alignment of the molecules, i.e.,

the director. The motion of the director in the oscillating liquid crystal greatly depends on the liquid crystalline phase: In the nematic, the director can reorient, and in a sufficiently strong magnetic field  $\theta$  and accordingly the magnetic torque remain small, and the frequency is essentially that of the pendulum. On the other hand, in the smectic *A*, the director oscillates with the sample, and thus the magnetic torque raises the oscillation frequency. In a qualitative way, the oscillation frequency is a measure of the motional freedom of the director: Lower oscillation frequency indicates easy reorientation of the director, higher frequency a more rigid binding of the director. For a quantitative treatment, an equation of motion of the director has to be postulated, describing its behavior under an applied magnetic torque. Integration of the equation must in general be done numerically on a computer. Such a calculation has for instance been made for a model of the smectic *C*,<sup>5</sup> but for our present discussion, the simplified treatment presented in the next section suffices.

## RESULTS

An overview of the results is given in Fig. 4. In this figure the pulse length (which is directly proportional to the damping) is given as function of temperature. The stability ranges of the different liquid crystalline phases is indicated at the top of the figure. It is obvious that dramatic changes in damping behavior occur at the phase transitions. These changes are directly correlated with the structure of the various phases. We shall discuss each of the phases in turn.

Referring to Fig. 4, it will be seen that a small damping is present in the crystalline phase (at the low end of the temperature range), as well as in the isotropic fluid (at the high end of the temperature range). This damping is predominantly due to external air damping of the oscillator. Other contributions to the damping are discussed in the Appendix. In the temperature range under consideration, the viscosity of air varies approximately as the square root of the temperature, and this fits the observed slight increase in damping on going from 50 to 280°C. Accordingly, we have interpolated the dotted line connecting these points in Fig. 4 and taken it as the background damping. The distance of a measured point above this line is then the damping due to the liquid crystal.

In the nematic phase, the director remains essentially aligned with the strong magnetic field, while under the conditions of the experiment the orbital motion of the liquid nearly follows the

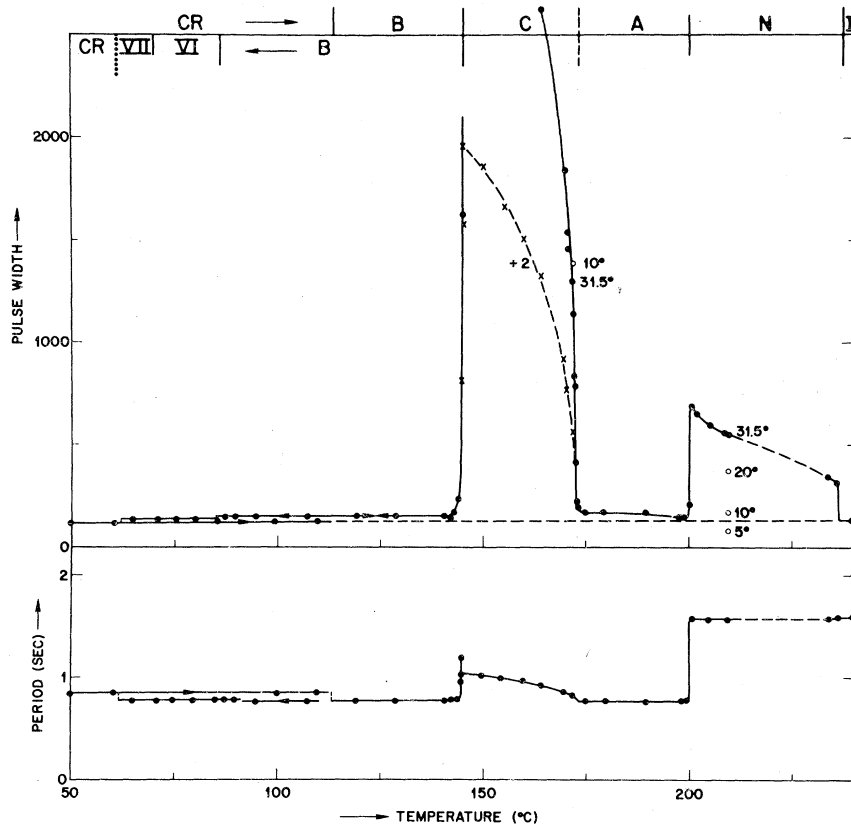


FIG. 4. In the upper part, the pulse length is plotted as a function of temperature. The temperature ranges of the different liquid crystalline phases are indicated at the top of the figure. The curve is for an oscillation amplitude of 31.5°; a few points at lower amplitudes are indicated by the open circles. The conversion of pulse length into dissipation is described in the data reduction section of the text; the unit of pulse length used in the graph is about 5  $\mu$ sec. The lower part of the figure gives the oscillation period, in seconds, on the same temperature scale.

oscillations (see Appendix). Any damping above the background is thus due to the rotational viscosity, characterized by the coefficient  $\gamma_1$ . Values for  $\gamma_1$  are easily obtained: In the nematic phase the frictional term is proportional to the angular velocity and the sample volume ( $V$ ), and the equation of motion of the oscillator becomes

$$I\ddot{\phi} + \gamma_1 V \dot{\phi} + \Gamma\phi = f(t). \tag{9}$$

Thus the dissipation is given by

$$D = 1/Q = \gamma_1 V / \omega I, \tag{10}$$

where  $\omega$  is defined by Eq. (7). Using Eq. (6), and the value of  $C$  given in the preceding section, one finds at the low-temperature end of the nematic range, at 202°C,  $\gamma_1 = 0.57$  P; while at the high end, at 235°C,  $\gamma_1 = 0.19$  P.

In the smectic-A phase the damping is much smaller than in the nematic, though it is not quite zero (see Figs. 4 and 5). It is known from the

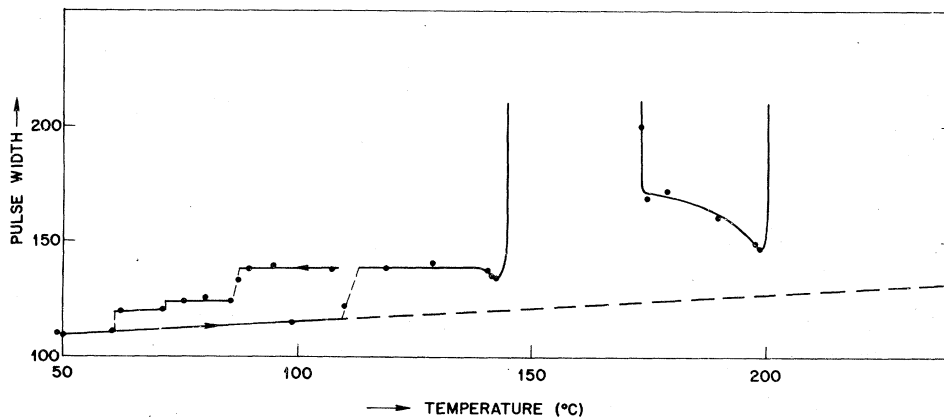


FIG. 5. Pulse length as function of temperature. This figure gives the data of the upper part of Fig. 4 on an expanded scale, to show the behavior in the phases with low damping.

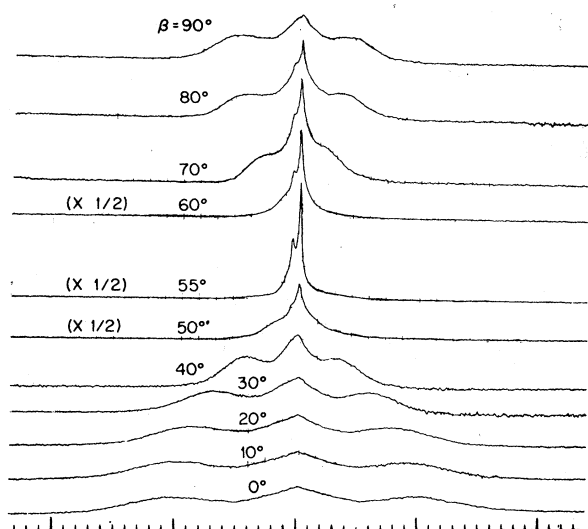


FIG. 6. NMR spectra of TBBA in the smectic-A phase (175 °C) as function of orientation with respect to magnetic field. This figure is taken from Ref. 7.

NMR spectrum<sup>6-8</sup> that the smectic planes are rigidly connected to the container: Figure 6 gives the behavior of the NMR spectrum on rotation of the sample. It is seen that the spectrum width goes according to the  $(3 \cos^2 \theta - 1)$  law, where  $\theta$  is the angle between the director and the magnetic field. It should be noted that, at a given angle  $\theta$ , the NMR spectrum does not change with time, for periods of at least a few hours. Thus it can be concluded that there is no measurable relaxation of the director orientation. If the smectic-A structure were completely rigid and anchored at the container walls, no damping (above the background) would be present. In fact, it is seen from Figs. 4 and 5 that some damping is present. At this stage the origin of this damping is unclear. One explanation considered is that the smectic layers remain completely rigid, but that the director can rotate slightly away from the normal to the planes. Such an effect has in fact been discussed by de Gennes.<sup>18</sup> It consists of a softening of the orientational rigidity of the director as the second-order phase transition to the smectic-C phase is approached. One expects a very small effect over most of the temperature range, and a critical divergence as the transition point is approached. De Gennes<sup>18</sup> estimates for the amplitude of the director deviation a magnitude of  $3 \times 10^{-4}$  rad ( $\approx 0.02^\circ$ ) at a temperature 1 °C above the transition for a magnetic field of 10 kG. This number would diverge as the transition point is approached with a critical exponent of 1.30. With these numbers, and assuming a

viscosity coefficient similar to that for the nematic, one estimates that a dissipation of the magnitude of the observed one occurs at a temperature about 0.02 °C above the transition point. Although this may be an observable effect, the measured damping does not show the critical behavior, and thus cannot be interpreted in this way.

The explanation of the observed damping must, therefore, necessarily involve a motion of the smectic planes. It is easy to see that if no disclinations are present and the ends of the smectic planes are solidly anchored to the container, then the planes will not distort on rotation of the magnetic field away from the normal to the planes: any distortion of the planes would result in an increase of magnetic energy. The damping mechanism must involve some motion of disclinations, which are no doubt present. It must be a limited motion, as the NMR results show that no long-term relaxation is observed within the sensitivity of those measurements which can be estimated at  $1^\circ$ – $2^\circ$ . However, at this time, we have no evidence that points to a specific model for the process.

The change in frequency when going from nematic to smectic A is a measure for the anisotropy of the magnetic susceptibility in the smectic-A phase. The frequency is given by Eq. (7). In the nematic,  $\Gamma$  equals the restoring torque of the suspension, which we indicate by  $\Gamma_0$ . In the smectic A, for small amplitudes, Eq. (8) gives

$$\Gamma = \Gamma_0 + \chi_a WH^2. \quad (11)$$

Combining Eqs. (7) and (11) gives

$$\chi_a = I(\omega_A^2 - \omega_0^2)/WH^2, \quad (12)$$

where  $\omega_A$  and  $\omega_0$  are the oscillation frequencies in, respectively, the smectic-A and nematic phases. One finds for the susceptibility anisotropy of the smectic A per gram

$$\chi_a = 4.32 \times 10^{-7} \text{ cgs.}$$

Referring again to Fig. 4, it is seen that in the smectic-C phase the damping increases as the temperature is lowered. The reason is that in this phase the direction of alignment of the long axis of the molecules becomes inclined to the smectic planes and thus acquires a degree of freedom—rotation about the normal to the planes—which is lacking in the smectic A. When the magnetic field rotates relative to the sample, the long axes of the molecules will reorient so as to make the magnetic energy a minimum, i.e., their direction will make as small an angle as possible with the magnetic field, consistent with the prescribed angle with the smectic planes. As in the smectic A, there is good NMR evi-

dence<sup>6-8</sup> that the smectic layers are "solid," that is, do not appreciably change their orientation with changes of field orientation. This model of the smectic *C* has been elaborated in previous papers<sup>6-8</sup> and a computer program has been written which integrates the equation of motion of the director. However, the following simple qualitative discussion gives a better insight into the behavior than a numerical computation will.

The transition from smectic *A* to smectic *C* is second order, and therefore just below the transition point the angle of inclination  $\theta$ , and thus the range over which the molecules can move, is small, much smaller than the amplitude  $A$  of the oscillation. The energy dissipation is proportional to

$$E_{\text{visc}} \propto (\text{torque}) \times (\text{angle}).$$

Now the viscous torque  $T$  is proportional to a viscosity coefficient  $\gamma$ , and to the angular velocity; the latter is in turn proportional to amplitude times frequency ( $\omega A$ ). The angle through which the director can move is proportional to the inclination angle  $\theta$ . Thus

$$E_{\text{visc}} \propto \gamma \omega A \theta. \quad (13)$$

This viscous energy loss is made up by the energy delivered by the current pulse, which is, as discussed before [Eq. (3)],

$$E_{\text{pulse}} \propto \omega A \tau. \quad (14)$$

As  $E_{\text{visc}} = E_{\text{pulse}}$  in the steady state, we find

$$\tau \propto \gamma \theta. \quad (15)$$

Note that this is independent of the amplitude and frequency! In Fig. 4 a number of experimental points with different amplitude are indicated by open circles, and it is seen that the pulse length is indeed independent of amplitude in the smectic-*C* phase.

It is instructive to do the same calculation for the nematic. There the director follows the magnetic field, and thus

$$\begin{aligned} E_{\text{visc}} &= (\text{torque}) \times (\text{angle}) \\ &\propto \gamma \omega A \times A \propto \gamma \omega A^2. \end{aligned} \quad (16)$$

The same argument as above gives

$$\tau \propto \gamma A \quad (17)$$

as is indeed found experimentally: in Fig. 4 the pulse length is proportional to amplitude for the nematic.

It is of interest to look at the decay behavior in the absence of a driving force for the two cases discussed above. We denote by  $A_1$  and  $A_2$  the amplitudes of two successive periods. The stored

energy is of course proportional to the square of the amplitude, and the decrease in stored energy must equal the viscous energy loss: For the nematic

$$\begin{aligned} A_1^2 - A_2^2 &\propto \gamma \omega [(A_1 + A_2)/2]^2, \\ A_1 - A_2 &\propto \gamma \omega \frac{1}{4} (A_1 + A_2). \end{aligned} \quad (18)$$

Thus the decrease in amplitude is proportional to the average amplitude—i.e., the decay is exponential, as indeed expected and observed for the nematic (Fig. 3).

The same calculation for the smectic *C* gives

$$\begin{aligned} A_1^2 - A_2^2 &\propto \gamma \omega \frac{1}{2} (A_1 + A_2) \theta, \\ A_1 - A_2 &\propto \gamma \omega \theta / 2. \end{aligned} \quad (19)$$

Thus the decrease in amplitude is independent of the amplitude of the oscillation, and the decay is linear—as indeed observed (Fig. 7). (The linearity of course breaks down when the oscillation amplitude  $A$  becomes comparable to the angle  $\theta$ .)

Equation (15) shows that the pulse length  $\tau$  can serve as a direct measure of the inclination angle  $\theta$  (the order parameter for the transition), provided we neglect the temperature variation of the viscosity  $\gamma$ . This may be a reasonable approximation over the narrow temperature range (less than two degrees) over which we shall apply the relation. Figure 8 shows the behavior of the pulse length ( $\tau$ ) near the transition of smectic *A* to smectic *C*. The larger plot shows the actual measurements; the scatter of the points suggests a reproducibility of the temperature of a few hundredth of a degree. The inset gives a log-log plot of  $\tau - \tau_0$  vs  $T_c - T$  ( $\tau_0$  is taken equal to the pulse length in the smectic *A*; and the transition temperature was taken from the first graph as 173.75°C). The slope of the log-log plot gives

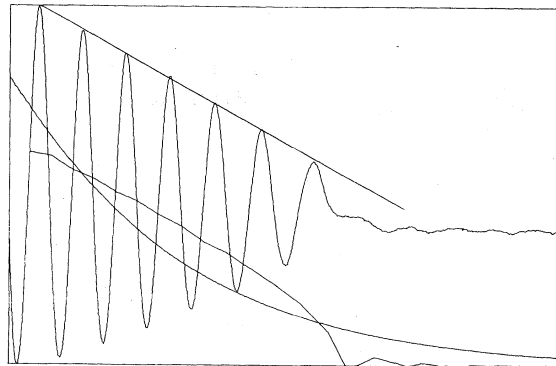


FIG. 7. Free decay of the pendulum when the sample is in the smectic-*C* phase. The temperature is 172.48°C. Other details as for Fig. 3.

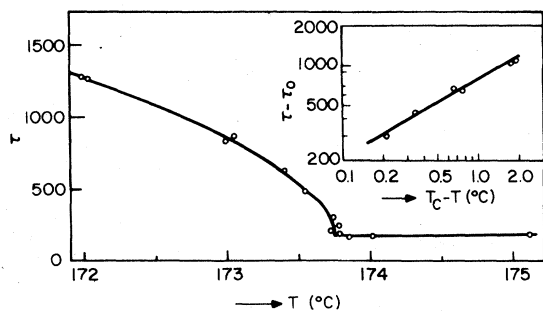


FIG. 8. Pulse length as function of temperature near the smectic-A to smectic-C transition. The large graph shows the experimental points. The inset is a log-log plot of these data, in which the pulse length of the smectic A has been taken as background, and subtracted from the smectic-C data; the temperature axis is relative to the transition temperature (173.75°C).

a critical exponent of 0.58. If we allow for a temperature dependence of the viscosity similar to that of the nematic (a change by a factor of about 2 for a change of 20° in temperature), then the exponent is reduced to 0.55. This seems compatible with a slope of 0.5 expected from mean-field theory. On the other hand, de Gennes<sup>18</sup> has pointed out that, as the relevant order parameter has two components (the magnitude of the inclination  $\theta$  and its azimuth), one expects a helium-like behavior and an exponent of 0.35. This is not borne out by the present results.

Finally, we have a few remarks regarding the low-temperature phases, the smectic  $B_c$  (also denoted as  $H$ ) and the metastable VI and VII phases. It will be seen from Figs. 4 and 5 that, like in the smectic A, a small but definite dissipation above the background is observed in these phases. Here too, the mechanism of the dissipation is unclear, but probably related to the motion of dislocations. The dissipation is halved in going from the  $B$  to the VI phase, and a small step can also be seen between the VI and VII phases (although the latter is not much above the precision of the measurements). It should be noted that these changes are reversible and can be reproduced on increasing temperature, as long as no crystallization has taken place. Once crystallization has occurred, heating to the melting point is of course required to effect a transition to the smectic  $B$ , as indicated by the arrows in the figures.

Another notable point is the behavior of the oscillation frequency. Referring to the lower graph of Fig. 4, it is seen that the period in the  $B$ , VI, and VII phases is the same as in the smectic A. This must mean that in the low-temperature phases, all the molecules are still

aligned very nearly parallel, as they are in the smectic A. This is in contrast to the crystalline state, in which the period is clearly longer than in the smectic phases. Thus part of the molecular alignment is lost on crystallization. This could be due to the fact that there is a distribution in the alignment of the crystallites, or, more probably, that there are molecules of different orientation in the unit cell of the crystal. The latter seems indicated by the fact that, when a sample is remelted into the smectic- $B$  phase, the period drops to the same value as observed for that phase after cooling from the nematic in a magnetic field. The described behavior is indicated by the arrows on the curves in Fig. 4.

## CONCLUSION

It has been shown that the temperature behavior of the rotational dissipation can be correlated with the structure of the various smectic phases. In particular, the high dissipation in the smectic C is the direct result of the internal degree of freedom that is characteristic of this phase. It should be stressed that the decay behavior of the smectic C indicates that the torque required to change director orientation is directly proportional to the *rate of change* of orientation [Eq. (13)]. This means that it is a viscous torque, characteristic of a liquid. Thus in this sense too the smectic-C layers can be appropriately denoted as a two-dimensional liquid.

As discussed in the preceding section, the critical exponent for the temperature dependence of the order parameter in the smectic-C phase just below the transition from the smectic A was found to be about 0.55, in much better agreement with mean-field theory than with the heliumlike model suggested by de Gennes.<sup>18</sup> Recently the same conclusion was reached by Delaye and Keller,<sup>19</sup> who used Rayleigh scattering to measure the critical fluctuations in the smectic-A phase of undecylazoxymethylcinnamate very near the smectic-A to smectic-C transition.

Mention should also be made of two papers which report on the temperature dependence of the smectic-C inclination angle in TBBA over a wide temperature range. They find agreement with power law with exponents of 0.40 (Ref. 6) and 0.34 (Ref. 20). However, these exponents are mainly based on measurements well away from the transition, and are therefore not characteristic of critical behavior.

The small damping observed in the smectic-A and B phases remains unexplained. It is hoped that a recent modification of the apparatus, in which the pendulum can be operated in a vacuum

so as to reduce background damping, will contribute to its elucidation.

#### ACKNOWLEDGMENT

We are indebted to Dr. Zeev Luz for the synthesis of the TBBA.

#### APPENDIX

We shall estimate the magnitude of two contributions to the oscillator damping: (i) eddy currents induced in the suspension and coil and (ii) viscous flow in the sample when it is in the liquid state.

We consider a torsional harmonic oscillator, of moment of inertia  $I$ , angular frequency  $\omega$ , and amplitude  $A$ . The angular position is

$$\alpha = A \sin \omega t. \quad (\text{A1})$$

We wish to estimate the quality factor  $Q$  which is conventionally defined by

$$Q = 2\pi \frac{(\text{stored energy})}{(\text{energy loss per period})}. \quad (\text{A2})$$

The stored energy equals the maximum kinetic energy:

$$E_{\text{stored}} = \frac{1}{2} I (\dot{\alpha})_{\text{max}}^2 = \frac{1}{2} I A^2 \omega^2. \quad (\text{A3})$$

(i) To estimate the eddy current losses, we consider a conducting loop of area  $S$  and total resistance  $R$ . As the loop oscillates in the magnetic field  $B$ , the magnetic flux through the loop is given by (we assume small oscillation amplitude)

$$\Phi = BSA \sin \omega t \quad (\text{A4})$$

and the induced voltage is

$$e_{\text{ind}} = \frac{d\Phi}{dt} = -BSA\omega \cos \omega t. \quad (\text{A5})$$

The average power dissipation of the resulting current is

$$(e_{\text{ind}})_{\text{max}}^2 / 2R = (BSA\omega)^2 / 2R \quad (\text{A6})$$

and the energy loss per cycle

$$E_{\text{loss}} = (BSA\omega)^2 (2\pi / 2R\omega). \quad (\text{A7})$$

Thus

$$Q = 2\pi (E_{\text{stored}} / E_{\text{loss}}) = IR\omega / B^2 S^2. \quad (\text{A8})$$

There are two current loops in the setup: (a) the detection coil, which is shunted by the input impedance of the amplifier and by that of the phototransistor bridge and, (b) the loop formed by the ribbon itself.

Estimating the contribution of (a), we have  $I = 0.0747 \text{ g cm}^2 = 7.47 \times 10^{-9} \text{ kg m}^2$ ,  $B = 13.2 \text{ kG}$

$= 1.32 \text{ T}$ ,  $S \approx 4 \times 10^{-4} \text{ m}^2$ ,  $\omega \approx 2\pi \text{ sec}^{-1}$ , giving  $Q \approx 0.2R$ . It is therefore necessary to keep the shunting resistance of the coil high. In practice it is about  $100 \text{ k}\Omega$ , giving a  $Q$  of about  $20\,000$ —a negligible contribution.

In order to estimate the order of magnitude of the contribution of the ribbon, we consider it as equivalent to a loop of width one half the ribbon width, length equal to ribbon length, and resistance 4 times ribbon resistance. The ribbon has a width of  $0.011 \text{ cm}$ , length of  $30 \text{ cm}$ , and resistance for that length of  $50 \Omega$ . Thus

$$Q = IR\omega / B^2 S^2 = 5000.$$

The above calculation is for the worst case that the plane of the ribbon is parallel to the magnetic field in the equilibrium position. In the actual setup the plane is about perpendicular to the field so that the actual damping is in fact smaller than the above figure.

(ii) We wish to calculate the damping due to the combined action of inertia and viscous flow in a cylindrical sample of radius  $R$ . As we are only interested in orders of magnitude, we simplify the problem by considering all the inertia concentrated in an effective rigid cylinder of radius  $aR$  (where  $0 < a < 1$ ), while the viscous flow takes place in the surrounding annulus between the cylinder (of radius  $aR$ ) and the container wall (of radius  $R$ ). The value of  $a$  is chosen to maximize the damping, and will be shown to be  $0.73$ .

We consider a harmonic oscillation of the container, its positional angle  $\alpha$  being given by

$$\alpha = A e^{i\omega t}. \quad (\text{A9})$$

We denote the position of the inertial cylinder relative to the container by the angle  $\beta$ , i.e.,  $\beta$  is the "slip" of the cylinder relative the container. The equation of motion of the inertial cylinder is then

$$I_c (\ddot{\alpha} + \ddot{\beta}) - V \dot{\beta} = 0. \quad (\text{A10})$$

Here  $I_c$  is the moment of inertia of the cylinder,

$$I_c = \rho (aR)^4 l / 4 \quad (\text{A11})$$

and  $V$  is the viscous drag torque:

$$V = 2\pi \left( \frac{1+a}{2} \right)^3 \frac{1}{1-a} R^2 l \eta. \quad (\text{A12})$$

In these equations  $\rho$  is the density of the sample,  $l$  its length, and  $\eta$  its viscosity. In writing the viscous term, the curvature of the annulus has been neglected for simplicity, and an average radius of  $\frac{1}{2}(1+a)R$ , and a thickness of  $(1-a)R$  for the layer is used.

The steady-state solution of Eq. (A10) can be written

$$\beta = P e^{i\omega t}, \quad (\text{A13})$$

and by substitution of (A13) and (A9) into (A10) one finds

$$P/A = 1/(1 + iV/I_c \omega). \quad (\text{A14})$$

The phase angle between  $P$  and  $A$  is given by

$$\cos \varphi = 1/[1 + (V/I_c \omega)^2]^{1/2}. \quad (\text{A15})$$

We again use Eq. (A2) to calculate the damping. The energy loss over a period is the integral of the viscous torque,  $V\dot{\beta}$ , with respect to the angle  $\alpha$ . The result of this integral is

$$(\text{energy loss per period}) = \frac{2\pi}{\omega} \omega^2 V \frac{|A| |P|}{2} \cos \varphi. \quad (\text{A16})$$

The maximum kinetic energy is

$$\frac{1}{2} I \left( \frac{d\alpha}{dt} \right)_{\max}^2 = \frac{1}{2} I \omega^2 |A|^2, \quad (\text{A17})$$

where  $I$  is the moment of inertia of the pendulum.

Thus, using Eqs. (A14)–(A17)

$$Q = 2\pi \frac{E_{\text{stored}}}{E_{\text{loss}}} = \frac{\omega I}{V} \left[ 1 + \left( \frac{V}{I_c \omega} \right)^2 \right]. \quad (\text{A18})$$

If  $\omega \gg V/I_c$ ,  $Q \approx \omega I/V$  and damping increases with frequency. If  $\omega \ll V/I_c$ ,  $Q \approx IV/I_c^2 \omega$  and damping decreases with frequency. The latter case applies here, as can be seen by substituting the numerical values quoted below. Substituting (A11) and (A12), one obtains for this case

$$Q \approx \frac{I}{I_c} \frac{\pi(1+a)^3}{a^4(1-a)} R^{-2} \eta \rho^{-1} \omega^{-1}. \quad (\text{A19})$$

The value of  $a$  for which this expression is minimum is obtained by differentiation. One finds  $a = 0.73$ .

In the actual experiment the values are  $R = 0.115$  cm,  $\omega \approx 2\pi \times 0.6$  sec<sup>-1</sup>,  $\eta \approx 1$  P,  $\rho \approx 1$ ,  $l \approx 1.2$  cm,  $I = 0.0747$  g cm<sup>2</sup>. Substitution gives  $Q \approx 2.1 \times 10^6$ . This is indeed negligible.

<sup>1</sup>If the molecular environment has a threefold or higher axis of symmetry, a unique director can be defined as this axis. In other cases the definition has some degree of arbitrariness. See, for instance, Ref. 2, p. 314.

<sup>2</sup>P. G. de Gennes, *The Physics of Liquid Crystals* (Oxford U. P., Oxford, 1975).

<sup>3</sup>V. Zwetkoff (V. N. Tsvetkov), *Acta Physicochim. URSS* **10**, 555 (1939).

<sup>4</sup>F. M. Leslie, *Q. J. Mech. Appl. Math.* **19**, 357 (1966).

<sup>5</sup>S. Meiboom and R. C. Hewitt, *Phys. Rev. Lett.* **34**, 1146 (1975).

<sup>6</sup>R. A. Wise, D. H. Smith, and J. W. Doane, *Phys. Rev. A* **7**, 1366 (1973).

<sup>7</sup>Z. Luz and S. Meiboom, *J. Chem. Phys.* **59**, 275 (1973).

<sup>8</sup>A. Luz, R. C. Hewitt, and S. Meiboom, *J. Chem. Phys.* **61**, 1758 (1974).

<sup>9</sup>J. Charvolin and B. Deloche, *J. Phys. (Paris)* **37**, C3 (1976).

<sup>10</sup>B. Deloche, J. Charvolin, L. Liébert, and L. Strze-

lecki, *J. Phys. (Paris)* **36**, C1 (1975).

<sup>11</sup>J. Doucet, A. M. Levelut, and M. Lambert, *Phys. Rev. Lett.* **32**, 301 (1974).

<sup>12</sup>A. M. Levelut and M. Lambert, *C. R. Acad. Sci. B* **272**, 1018 (1971).

<sup>13</sup>T. R. Taylor, S. L. Arora, and J. L. Ferguson, *Phys. Rev. Lett.* **25**, 722 (1970).

<sup>14</sup>H. Hervet, F. Volino, A. J. Dianoux, and R. E. Lechner, *J. Phys. Lett.* **35**, L151 (1974).

<sup>15</sup>J. M. Schnur and M. Fontana, *J. Phys. Lett.* **35**, L53 (1974).

<sup>16</sup>D. Dvorjetski, V. Volterra, and E. Wiener-Avneer, *Phys. Rev. A* **12**, 681 (1975).

<sup>17</sup>R. M. Hornreich and S. Shtrikman, *Solid State Commun.* **17**, 1141 (1975).

<sup>18</sup>P. G. de Gennes, *C. R. Acad. Sci. B* **274**, 758 (1972).

<sup>19</sup>M. Dalayé and P. Keller, *Phys. Rev. Lett.* **37**, 1065 (1976).

<sup>20</sup>P. J. Flanders, *App. Phys. Lett.* **28**, 571 (1976).